

A disturbing view of life history evolution

Katie Murray¹, Stuart Townley² and Dave Hodgson^{1,*}

¹Centre for Ecology and Conservation, Faculty of Environment, Science and Economy, University of Exeter, Penryn Campus, Penryn, Cornwall UK

²Department of Earth and Environmental Sciences, and Environment and Sustainability Institute, Faculty of Environment, Science and Economy, University of Exeter, Penryn Campus, Penryn, Cornwall UK

*Corresponding author, email d.j.hodgson@exeter.ac.uk

Author Contributions: DH conceived the ideas and performed initial models; ST guided the mathematics and theory; KM performed the models and created the visuals. All authors wrote the manuscript.

Data Accessibility Statement: Simulation code and figures are archived with Dryad, available for review at https://datadryad.org/stash/share/EXhph-nk1_w5pUFyPjR3iITQAdSdOhbCv0IsCQigx6s. On acceptance the files will be hosted at doi:10.5061/dryad.8931zcs02

Keywords: life history, demography, disturbance, fitness, stochastic, evolution, resilience, resistance, recovery

Type of Article: Letter

Words in Abstract: 150

Words in Main Text: 3313

Number of References: 45

Number of Figures: 6

23 **Number of Tables and text boxes: 0**

24 **To whom Correspondence should be sent:** Professor Dave Hodgson, Centre for
25 Ecology and Conservation, Faculty of Environment, Science and Economy,
26 University of Exeter, Penryn Campus, Penryn, Cornwall, UK TR10 9FE.

27 **Telephone: +44 1326 371829**

28 **Email:** d.j.hodgson@exeter.ac.uk

29

Abstract

Species' lifetime schedules of survival, growth and reproduction generally assort along a principal axis called the "fast-slow" continuum, with positions attributed to the value of producing many, fragile offspring early, versus few, high-quality offspring later. Fast species are classically associated with surplus or pulsed resources, and slow species with stable, limiting resources. Here we demonstrate that the fast-slow continuum emerges as a zone of highest fitness in the face of random, structured demographic disturbances, regardless of resource supply, competition, or life history trade-offs. Our resilience framework measures resistance, recovery, and fitness of stage-structured life histories in disturbed environments. Random disturbances favour either fast or slow life history variants due to their respective weak resistance and fast recovery, or strong resistance and slow recovery. Demographic disturbance regimes are important in shaping nature's diversity of life histories, and the resilience framework is a useful tool for understanding species' responses to environmental change.

50 **Introduction**

51 The life history of any individual organism is its lifetime schedule of survival, growth
52 and reproduction; the life history of a genotype, population or species is summarised
53 as statistics describing the expected lifetime schedule of its constituent members
54 (Stearns 1998). Life history associates with fitness, because natural selection
55 favours schedules of survival and reproduction that maximise numerical
56 representation in future generations. Life histories also associate with ecological
57 features of species, including extinction risk (Purvis *et al.* 2000, Hutchings *et al.*
58 2012), invasiveness (Hamilton *et al.* 2005, Jelbert *et al.* 2015), crop yields (Mifflin
59 2000) and ecosystem function (Jeppesen *et al.* 2010, Adler *et al.* 2014). For these
60 reasons, a great deal of effort has been invested in understanding the diversity of life
61 histories found in nature. Prevailing schools of thought have converged on theory
62 and observation that collapses most life history variation along a principal axis of
63 variation, from “fast” to “slow” (Stearns 1983, Franco and Silvertown 1996, Salguero-
64 Gómez *et al.* 2016). Secondary axes of variation are observed in several broad taxa
65 (Bielby *et al.* 2007, Salguero-Gómez *et al.* 2016), but to date, theory and observation
66 agree on the features of the main axis. Fast species invest in rapid maturation and
67 the production of large numbers of offspring, at the expense of survival and somatic
68 maintenance. Slow species invest in survival and maintenance, producing small
69 numbers of offspring that tend to survive.

70 Formal theory explains the fast-slow continuum in terms of selection pressures
71 acting on the timing and magnitude of reproductive output (Stearns 1998), coupled
72 with presumed trade-offs between maintenance and reproduction (Stearns 1983). In
73 stable environments, investment in survival and self-maintenance, at the expense of
74 early reproduction, can be favoured if it results in increased lifetime reproductive

output (Cole 1954, Gadgil and Bossert 1970, Bell 1980, Roff 1981). If the population is growing, this increase must also exceed the inflationary costs of delayed reproduction (future offspring will be worth less, per capita, than current ones).

Furthermore, when adults survive better than juveniles, iteroparity (the repeated production of offspring through an extended reproductive lifespan) is favoured over semelparity (single-bout or “big bang” reproduction, followed by death) (Gadgil and Bossert 1970, Charnov and Schaffer 1973, Stearns 1998).

A recent synthesis (Wright *et al.* 2019), which aligns fast-slow thinking with classical r-K theory (MacArthur 1962, Boyce 1984, Lande *et al.* 2017), argues that the relative success of fast versus slow life histories is mediated by density-dependent selection, with fast favoured by surplus resources in small populations, and slow favoured under competition for limited resources. This theory aligns well with observation: species like aphids scramble for predictably pulsed resources, reproducing rapidly to maximise fitness during rapid population growth; while elephants invest heavily in survival and somatic maintenance, achieving large body size that helps them compete for limiting but reliable resources, replacing themselves by producing small numbers of high-quality offspring over long lifespans.

In environments that offer unpredictable, fluctuating resources, fitness benefits of longer lifespans can be amplified by spreading the risk of reproduction through time (Tuljapurkar 1990), despite the associated costs of somatic maintenance and survival. These benefits are gained because geometric mean fitness increases with arithmetic mean fitness but decreases with its variance (Gillespie 1977). Extreme environmental fluctuations can favour extreme bet-hedging life histories like diapausing egg stages of water fleas and seed dormancy in many plants (Evans and Dennehy 2005), but the adaptive benefits of life-history buffering or lability

(McDonald *et al.* 2017) can favour a range of life history strategies in unpredictable environments (Wilbur and Rudolf 2006). In semelparous species (in which reproduction and death coincide), delayed reproduction can be favoured among slow species when fertility varies through time, and among fast species when survival varies (Koons *et al.* 2008).

Overall, prevailing wisdom suggests that selection pressures on life-history strategies arrange species along a fast-slow continuum, with their positions depending first on the relationship between age-specific survival, development and reproductive output (Stearns 1998), then on a combination of intensity of competition for limited resources (Wright *et al.* 2019), environmental uncertainty and current position on the fast-slow axis (Koons *et al.* 2008).

Here we offer an alternative to that synthesis, proposing instead that random demographic disturbances alone can impose the selection pressures that generate the fast-slow life history continuum in the first place.

In stable environments with surplus resources, stage-structured populations settle to a stable stage structure with a stable rate of increase (Caswell 2000). The stable structure and dynamic are determined by stage-specific probabilities of survival and rates of reproduction, i.e. by the vital rates that comprise the organism's life history. Stage-structured disturbances harm different life histories differently (Stott, Townley and Hodgson 2011, White *et al.* 2022, Appendix 1), hence life histories vary in their resistance to disturbance. When demographic disturbances knock populations away from their stable structure, transient dynamics are invoked that differ from the stable rate of increase (Stott *et al.* 2011), hence life histories also vary in their recovery from disturbance (Appendix 2). Resistance and recovery are the two main

components of engineering resilience (Holling 1996, Hodgson *et al.* 2015), and here we show that the differential resilience of stage-structured life histories determines the fitness value of fast, slow and other strategies in the face of random, structured, demographic disturbances.

Methods

We consider simple life histories with any possible combination of stage-specific survival and reproduction, subject to the constraint that their fitnesses in undisturbed environments, i.e. their stable rates of increase, are identical. In a stable environment with unlimited resources, these life histories are equally fit. We then subject populations to demographic disturbances that are random in their timing, structure and magnitude, serving as a type of time-varying environmental model (Caswell, 2000). But, our approach to environmental stochasticity differs from prevailing approaches in demographic research. Rather than introduce variation to the stage-dependent rates of survival and reproduction directly in the demographic system defined by the stage-structured projection matrix, we choose instead to implement removals from the population by culling random proportions of individuals from the state vector describing the abundance of each stage. This approach allows us to tease apart the resistance and recovery aspects of population responses (Hodgson *et al.*, 2015). In Supplementary Materials we show that the same outcomes are seen when disturbances are modelled into the demographic system.

Our simulation models are in discrete time, and disturbances occur with fixed probability per timestep. Our life histories are described as projection matrices composed of two stages, with four vital rates. In our first scenario, all surviving stage-1 individuals progress to stage-2 at the end of the first timestep, with stage-specific

survivals s_1 and s_2 and stage-specific productivities p_1 and p_2 . We call this the “structured reproduction” model. In our second scenario, we prevent stage-1 individuals from reproducing and introduce a maturation parameter ϕ , the per-timestep probability of progression from stage-1 to stage-2. We call this the “delayed maturation” model. In each scenario, three vital rates of the life history are free to vary while the fourth is constrained by the fixed stable rate of increase, which is the dominant eigenvalue of the projection matrix, λ_1 . The system is monitored post-reproductively, such that during any timestep, individuals survive then produce offspring then are counted. At any timestep and in the absence of disturbance, the vector of stage-specific abundances, \mathbf{x} , updates according to

$$\mathbf{x}_{t+1} = \mathbf{A}\mathbf{x}_t \quad \text{[Equation1]}$$

We introduce structured, random disturbance regimes to each scenario, by culling a random proportion of individuals from each lifestage, with the per-timestep flip of a weighted coin, f , prior to the processes of survival and reproduction. Extending the culling algebra of Hauser *et al.* (2006) and the harvesting algebra of Lefkovich (1967), we define the culling/disturbance matrix \mathbf{C}_t to contain the proportion of each stage class remaining following disturbance at time t :

$$\mathbf{C}_t = \begin{bmatrix} c_{1,t} & 0 \\ 0 & c_{2,t} \end{bmatrix} \text{ where } c_{i,t} = \begin{cases} Unif(0,1) & \text{if } Bernoulli(f) = 1 \\ 1 & \text{if } Bernoulli(f) = 0 \end{cases} \quad \text{[Equation2]}$$

When exposed to the risk of disturbance, the single timestep projection of the population vector becomes

$$\mathbf{x}_{t+1} = \mathbf{A}\mathbf{C}_t\mathbf{x}_t = \mathbf{A}_t^*\mathbf{x}_t = \begin{bmatrix} a_{1,1}c_{1,t} & a_{1,2}c_{2,t} \\ a_{2,1}c_{1,t} & a_{2,2}c_{2,t} \end{bmatrix} \mathbf{x}_t \quad \text{[Equation 3]}$$

Scenario 1: Stage-structured reproduction

Consider a two-lifestage model of juveniles and adults where adults survive with probability $0 < s_2 < 1$ and reproduce with fecundity $0 < p_2$, and where juveniles mature in one timestep with survival $0 < s_1 < 1$ and either cannot reproduce (i.e. $p_1 = 0$) or have productivity at the end of their first timestep of life ($0 < p_1 < 2$). We simulated life histories across all feasible combinations of s_1 , s_2 and p_1 that achieved a nominal stable rate of increase of 1.2. This choice of undisturbed fitness value is arbitrary, chosen to keep simulated populations approximately stable in the face of disturbance, but all our findings are robust to different choices. Juvenile and adult survivals were set to span from 0.05 to 1 in increments of 0.05, juvenile productivity to span a sequence from 0 to 2 and adult productivity was calculated from these and the PPM eigenvalue constraint ($\lambda_1 = 1.2$).

$$\mathbf{A} = \begin{bmatrix} s_1 p_1 & s_2 p_2 \\ s_1 & s_2 \end{bmatrix} \quad [\text{Equation 4}]$$

and the time-varying disturbed projection matrix is

$$\mathbf{A}_t^* = \begin{bmatrix} s_1 p_1 c_{1,t} & s_2 p_2 c_{2,t} \\ s_1 c_{1,t} & s_2 c_{2,t} \end{bmatrix} \quad [\text{Equation 5}]$$

Scenario 2: Delayed maturation

In this scenario we extend Scenario 1 by introducing a parameter φ governing the probability with which juveniles mature, i.e. transition from stage 1 to stage 2, and by preventing juveniles from reproducing ($p_1 = 0$), sometimes known as ‘coin-flipping maturation’. We simulated life histories across all feasible combinations of s_1 , s_2 , φ and p_2 that achieved the nominal stable rate of increase of 1.2.

192

193
$$\mathbf{A} = \begin{bmatrix} s_1(1 - \varphi) & s_2 p_2 \\ s_1 \varphi & s_2 \end{bmatrix} \quad [\text{Equation 6}]$$

194 And the time-varying disturbed projection matrix is

195
$$\mathbf{A}_t^* = \begin{bmatrix} s_1(1 - \varphi)c_{1,t} & s_2 p_2 c_{2,t} \\ s_1 \varphi c_{1,t} & s_2 c_{2,t} \end{bmatrix} \quad [\text{Equation 7}]$$

196

197 **Realised stochastic dynamics**

198 The abundance of each population at any timepoint is $n_t = \sum x_t$. Over any single
199 timestep, the geometric dynamic of each population is

200
$$\frac{\|x_{t+1}\|}{\|x_t\|} = \frac{\|A C_t x_t\|}{\|x_t\|} \quad [\text{Equation 8}]$$

201 Where $\|x\|$ is the one-norm, or column-sum, of the vector x . This geometric dynamic
202 can be re-expressed as the product of the two main components of resilience:

203 resistance, and recovery. Resistance is the proportion of the current population that

204 survives demographic disturbance ($d_t = \frac{\|C_t x_t\|}{\|x_t\|}$). While all simulated life histories are

205 exposed to disturbances with the same expected value of d_t , it is the relationship

206 between the stable stage structure and the variance in d_t that causes variation in

207 resistance (Appendix 1). The second component of resilience, recovery, has two

208 sub-components: the stable rate of increase λ_1 , and any extra, transient growth or

209 decline caused by deviation from stable stage structure (transient reactivity, $a_t =$

210 $\frac{\|A C_t x_t\|}{\lambda_1 \|C_t x_t\|}$ (Stott *et al* 2011)). We show the association between life-history parameters,

211 disturbed stage structure, and reactivity, in Appendix 2.

212 During a single timestep, the geometric change in abundance of a disturbed
 213 population can be expanded to describe the distinct processes of resistance and
 214 both stable and transient recovery:

$$215 \frac{\|x_{t+1}\|}{\|x_t\|} = \frac{\|AC_t x_t\|}{\|x_t\|} = \frac{\|C_t x_t\|}{\|x_t\|} \cdot \lambda_1 \cdot \frac{\|AC_t x_t\|}{\|C_t x_t\| \lambda_1} = d_t \lambda_1 a_t \quad [\text{Equation 9}]$$

216 Over multiple timesteps (T), the long-term stochastic rate of increase (λ_s , AKA
 217 fitness) is estimated as the geometric average of the temporal product of this
 218 product.

$$219 \hat{\lambda}_s = (\prod_{t=1}^T d_t \lambda_1 a_t)^{\frac{1}{T}} \quad [\text{Equation 10}]$$

220 Taking logs and denoting \hat{r}_s as our estimator of $\log(\lambda_s)$,

$$221 \hat{r}_s = \frac{\sum_{t=1}^T (\log(d_t) + \log(\lambda_1) + \log(a_t))}{T} = \frac{\log(n_T/n_0)}{T} \quad [\text{Equation 11}]$$

222 In each modelling scenario, we create life histories that span all possible
 223 combinations of stage-specific survival, productivity and /or maturation that, in the
 224 absence of disturbance, achieve a stable rate of increase of 1.2. We project each of
 225 these life histories from a starting density of 1, and initial structure equal to the stable
 226 stage structure (dominant right eigenvector) of the life history, for 1000 timesteps,
 227 disturbing each timestep with a probability of $f = 0.2$. We monitor \mathbf{x} , and therefore n ,
 228 per timestep for each projection. We replicate projections for each life history 100
 229 times. All results are robust to lengthening the duration of simulations (tested up to
 230 100,000 timesteps). All visualisations of stochastic fitness, resistance and recovery,
 231 are among-replicate averages of per-timestep averages of log-transformed rates of
 232 increase or decline.

Results are visualised using two-dimensional heatmaps, coloured by measurements of average recovery, resistance and stochastic growth rate \hat{r}_s , over all viable combinations of s_1 , s_2 , p_1 , p_2 and φ . Only two of the four parameters can appear on the bivariate axes, hence we describe a third parameter using panels, and use contours for the fourth (noting that each model includes a parameter constrained by constant λ_1). Plot shading is a purple-to-green gradient to indicate the magnitude of recovery, resistance or the stochastic growth rate from values low-to-high.

In Supplementary Materials we show that the same patterns in stochastic fitness are seen when disturbances are modelled into the demographic system (Equations 5 and 7).

Results

Model 1: Stage-structured productivity

This scenario introduces a constraint on parameter space because when $s_1 p_1$ exceeds 1.2, $\lambda_1 > 1.2$ so the nominal stable rate of increase is exceeded by the first lifestage alone. This constraint is seen as white space in the third row of panels in Figure 1, i.e. for large values of p_1 . We simulated life histories across all feasible combinations of s_1 , s_2 , p_1 and p_2 that achieved the nominal stable rate of increase of 1.2.

[Figure 1 HERE]

With increasing magnitude of yearling productivity, the zone of highest fitness shifts from a simple negative association between productivity and juvenile survival, to a more generalised negative association between productivity and survival (Figure 1). Highest fitness occurs along a ridge of increasing survival probabilities, with an associated decline in productivity, very much resembling the fast-slow continuum. Highest fitness is enjoyed by life histories with relatively high survival and moderate yearling productivity, and lowest fitness is suffered by life histories with very different yearling and adult rates of survival.

[Figure 2 HERE]

[Figure 3 HERE]

The patterns in fitness shown in Figure 1 are explained by associated patterns in resistance to, and recovery from, random demographic disturbances (Figures 2 and 3). Resistance is maximised along a ridge of negative association between yearling survival and adult survival, and for intermediate magnitudes of yearling productivity, this ridge lies along a contour of equal adult productivity. Recovery shows a very different saddle-shaped pattern with high rates of recovery among the fastest and slowest life histories and low rates of recovery for life histories with divergent stage-specific rates of survival. The combined effect of resistance and recovery yields the emergent patterns of stochastic growth in Figure 1.

In the special case where juvenile productivity is set to zero (i.e. juveniles are prevented from reproducing), demographic disturbance favours an optimal rate of adult survival, regardless of values of juvenile survival and adult productivity (top-left panel in Figure 1). The contours of productivity reveal a negative association with

juvenile survival along this ridge of highest fitness, implying a simple trade-off between the quality and quantity of juveniles. Underpinning this pattern is a clear negative association between the resistance of life histories to random disturbance regimes (top-left panel Figure 2), and rate of recovery from them (top-left panel Figure 3). Highest resistance lies along a ridge described by intermediate productivity and a negative association between adult survival and juvenile survival. Highest rates of recovery, meanwhile, are enjoyed by life histories with very low rates of juvenile survival, low-medium adult survival and medium-high productivity.

Model 2: Delayed Maturation

In this delayed-maturation model, demographic disturbances favour relatively low rates of maturation, and hence delayed reproduction, surrounded by a zone of high fitness resembling the fast-slow continuum, i.e. a negative association between rates of survival and of productivity (Figure 4). For high rates of maturation, the fitness patterns move towards the special case of zero juvenile productivity in Scenario 1, favouring moderate values of adult survival and a negative association between productivity and juvenile survival, but with one key difference: high juvenile survival and low productivity is favoured.

[Figure 4 HERE]

[Figure 5 HERE]

[Figure 6 HERE]

Patterns of resistance and recovery, for the delayed-maturation scenario, explain the observed patterns in fitness across the simulated life histories. Resistance is low among life histories that mature slowly, then is maximised along a ridge of negative association between juvenile survival and adult survival, with intermediate

magnitudes of productivity (Figure 5). Recovery is fastest among slow-maturing life histories, but as maturation rate increases, the life histories that achieve slowest recovery change from those with high juvenile survival to those with low juvenile survival (Figure 6).

Discussion

Using two simple life history scenarios, we have shown that the introduction of random, stage-structured disturbances, changes flat fitness surfaces into landscapes that favour an axis of life history variation closely resembling the fast-slow continuum. Generally, fast life histories that favour productivity and rapid maturation over survival, have weak resistance to unpredictable disturbances, but recover quickly. Meanwhile, slow life histories that favour survival over productivity and rapid maturation, are resistant to disturbances but recover slowly. Fitness, which integrates across resistance and recovery, is maximised for life histories along the fast-slow axis. Fundamentally, there is no need for differences among species in the frequency, intensity or structure of demographic disturbances to place those species along the fast-slow continuum: the continuum itself emerges as a contour of equal fitness in the face of stochastic disturbances. There is also no need for differences among species in the supply of resources or the ability to compete for them.

Life histories that deviate from this emergent fast-slow axis, for example by having very different rates of adult and juvenile survival, tend to perform badly in the face of random disturbances. On face value this is surprising because, in nature, variation in survival, among ages or stages, is prevalent. A simple explanation for natural patterns of age-structured mortality is the typical ontogeny of increasing size with

maturation – physical constraints require offspring to be smaller than their mothers, and survival often scales allometrically with size (Promislow 1993) – but other explanations for differences in age-specific survival might include the actual structure, amplitude and frequency of demographic disturbances experienced in nature (White *et al.* 2022). Perhaps natural disturbance regimes favour the production of atypically fragile (altricial) or robust (precocious) offspring. We note that a special case of both our modelling scenarios, when juveniles cannot reproduce and all individuals mature at the same age, favours a trade-off between productivity and juvenile survival and hence a dissociation of age-specific rates of survival. For this special case, further work is required to explain the observation that random disturbances favour a fixed adult survival, regardless of the values of juvenile survival and productivity.

When productivity is introduced for stage-1 individuals, the fitness value of survival rates in the two stages become aligned, and it is this lifetime survival rate that trades off against productivity to form the fast-slow continuum. This pattern is governed by opposing patterns of resistance and recovery, across life histories. The saddle-shaped recovery surface, highest for both high-productivity, low survival and for low productivity, high survival life histories, deserves further study. If stochastic fitness is linked strongly to rates of recovery, then this saddle-shape could describe divergent selection along the fast-slow continuum.

When we introduce variation in the rate of maturation, we find that the fast-slow axis is governed mainly by weak resistance but strong recovery in slow-maturing life histories and vice versa for fast-maturing life histories, while subtle variations in these patterns yield a ridge of highest fitness along the fast-slow continuum. The alignment of adult and juvenile survival, along this ridge, weakens as the rate of

maturation increases, however high rates of maturation have relatively low fitness, implying that stochastic disturbance is sufficient to favour delayed reproduction. If all juveniles mature in their first timestep, we return to the simple scenario that favours a negative association between quantity and quality of offspring.

Beyond this demonstration that random demographic disturbances can select for the fast-slow axis of life history variation, the resilience framework (Hodgson *et al.* 2015, Capdevila *et al.* 2020) has great potential for more detailed and mechanistic understanding of real-world life histories in disturbed environments. All natural populations have vital rates of survival and reproduction that vary through time, and it is not unusual for populations to be affected by structured demographic disturbances like fire (Caswell and Kaye 2001), flood (Smith *et al.* 2005), extreme weather (Abernathy *et al.* 2019), cull (Lachish *et al.* 2010) or epidemic (Benhaïem *et al.* 2018). Typically this variation is modelled using projection models containing age- or stage-specific vital rates that vary through time or among environments (Boyce *et al.* 2006, Tuljapurkar 2013). Our alternative, i.e. the use of fixed vital rates but with disturbances applied to stage structures, opens the large (and growing) toolbox of transient dynamic analysis (Stott *et al.* 2011), and lends itself to questions around the resistance of structured systems to disturbance regimes, and the subsequent rates of recovery.

Resilience in the face of disturbance is an increasingly important feature of natural systems in an era of anthropogenic environmental change (Hodgson *et al.* 2015). Life histories have evolved in disturbed environments since life began, and it is intriguing to observe that random demographic disturbance regimes can favour delayed reproduction, age-structured reproduction and the arrangement of life histories along the fast-slow continuum. Demographic resilience is a clear rival to the

classic explanations of why fast- and slow-living species coexist in nature. Natural populations are subject to a variety of structures, amplitudes and frequencies of demographic disturbances and it would be interesting to consider how natural selection has shaped, and will shape, the resilience of genotypes, populations and species to current and future disturbance regimes.

References:

- Abernathy, H. N., D. A. Crawford, E. P. Garrison, R. Chandler, M. Conner, K. Miller and M. J. Cherry (2019). Deer movement and resource selection during Hurricane Irma, implications for extreme climatic events and wildlife. *Proc. Roy. Soc. B* 286(1916), 20192230.
- Adler, P. B., R. Salguero-Gómez, A. Compagnoni, J. S. Hsu, J. Ray-Mukherjee, C. Mbeau-Ache and M. Franco (2014). Functional traits explain variation in plant life history strategies. *Proc. Nat Acad. Sci.* 111, 740-745.
- Bell, G. (1980). The costs of reproduction and their consequences. *Am. Nat.* 116, 45-76.
- Benhaïem, S., L. Marescot, M. L. East, S. Kramer-Schadt, O. Gimenez, J.-D. Lebreton and H. Hofer (2018). Slow recovery from a disease epidemic in the spotted hyena, a keystone social carnivore. *Commun. Biol.* 1, 201.
- Bielby, J., G. M. Mace, O. R. Bininda-Emonds, M. Cardillo, J. L. Gittleman, K. E. Jones, C. D. L. Orme and A. Purvis (2007). The fast-slow continuum in mammalian life history: an empirical reevaluation. *Am. Nat.* 169, 748-757.
- Boyce, M. S. (1984). Restitution of gamma-and k-selection as a model of density-dependent natural selection. *Ann. Rev. Ecol Syst.* 15, 427-447.

399 Boyce, M. S., C. V. Haridas, C. T. Lee and N. S. D. W. Group (2006). Demography
 400 in an increasingly variable world. *Trends Ecol. Evol.* 21, 141-148.
 401 Capdevila, P., I. Stott, M. Beger and R. Salguero-Gómez (2020). Towards a
 402 comparative framework of demographic resilience. *Trends Ecol. Evol.* 35,
 403 776-786.
 404 Caswell, H. (2000). Matrix population models, Sinauer Sunderland, MA.
 405 Caswell, H. and T. N. Kaye (2001). Stochastic demography and conservation of an
 406 endangered perennial plant (*Lomatium bradshawii*) in a dynamic fire regime.
 407 *Adv. Ecol. Res.* 32, 1-51.
 408 Charnov, E. L. and W. M. Schaffer (1973). Life-history consequences of natural
 409 selection, Cole's result revisited. *Am. Nat.* 107, 791-793.
 410 Cole, L. C. (1954). The population consequences of life history phenomena. The
 411 *Quart. Rev. Biol.* 29, 103-137.
 412 Evans, M. E. and J. J. Dennehy (2005). Germ banking, bet-hedging and variable
 413 release from egg and seed dormancy. *Quart. Rev. Biol.* 80, 431-451.
 414 Franco, M. and J. Silvertown (1996). Life history variation in plants, an exploration of
 415 the fast-slow continuum hypothesis. *Phil. Trans. Roy. Soc. B* 351, 1341-
 416 1348.
 417 Gadgil, M. and W. H. Bossert (1970). Life historical consequences of natural
 418 selection. *Am. Nat.* 104, 1-24.
 419 Gillespie, J. H. (1977). Natural selection for variances in offspring numbers, a new
 420 evolutionary principle. *Am. Nat* 111, 1010-1014.
 421 Hamilton, M. A., B. R. Murray, M. W. Cadotte, G. C. Hose, A. C. Baker, C. J. Harris
 422 and D. Licari (2005). Life-history correlates of plant invasiveness at regional
 423 and continental scales. *Ecol. Letts.* 8, 1066-1074.

424 Hauser, C., E. Cooch and J.-D. Lebreton (2006). Control of structured populations by
425 harvest. *Ecol. Model.* 196, 462-470.

426 Hodgson, D., J. L. McDonald and D. J. Hosken (2015). What do you mean, 'resilient'?
427 *Trends Ecol. Evol.* 30, 503-506.

428 Holling, C. S. (1996). Engineering resilience versus ecological resilience. In Schulze,
429 P. (Ed.) *Engineering within ecological constraints*. National Academies
430 Press.

431 Hutchings, J. A., R. A. Myers, V. B. García, L. O. Lucifora and A. Kuparinen (2012).
432 Life-history correlates of extinction risk and recovery potential. *Ecol. Appl.*
433 22, 1061-1067.

434 Jelbert, K., I. Stott, R. A. McDonald and D. Hodgson (2015). Invasiveness of plants is
435 predicted by size and fecundity in the native range. *Ecol. Evol.* 5, 1933-1943.

436 Jeppesen, E., M. Meerhoff, K. Holmgren, I. González-Bergonzoni, F. Teixeira-de
437 Mello, S. A. Declerck, L. De Meester, M. Søndergaard, T. L. Lauridsen and
438 R. Bjerring (2010). Impacts of climate warming on lake fish community
439 structure and potential effects on ecosystem function. *Hydrobiol.* 646, 73-90.

440 Koons, D. N., C. J. E. Metcalf and S. Tuljapurkar (2008). Evolution of delayed
441 reproduction in uncertain environments, a life-history perspective. *Am. Nat.*
442 172, 797-805.

443 Lachish, S., H. McCallum, D. Mann, C. E. Pukk and M. E. Jones (2010). Evaluation
444 of selective culling of infected individuals to control Tasmanian devil facial
445 tumor disease. *Cons. Biol.* 24, 841-851.

446 Lande, R., S. Engen and B.-E. Sæther (2017). Evolution of stochastic demography
447 with life history tradeoffs in density-dependent age-structured populations.
448 *Proc. Nat. Acad. Sci.* 114, 11582-11590.

449 Lefkovitch, L. (1967). A theoretical evaluation of population growth after removing
 450 individuals from some age groups. *Bull. Ent. Res.* **57**(3), 437-445.
 451 MacArthur, R. H. (1962). Some generalized theorems of natural selection. *Proc. Nat.*
 452 *Acad. Sci.* **48**, 1893-1897.
 453 McDonald, J. L., M. Franco, S. Townley, T. H. Ezard, K. Jelbert and D. J. Hodgson
 454 (2017). Divergent demographic strategies of plants in variable environments.
 455 *Nature Ecol. Evol.* **1**, 0029.
 456 Miflin, B. (2000). Crop improvement in the 21st century. *J. Exp. Bot.* **51**(342), 1-8.
 457 Promislow, D. E. (1993). On size and survival, progress and pitfalls in the allometry
 458 of life span. *J. Geront.* **48**, B115-B123.
 459 Purvis, A., J. L. Gittleman, G. Cowlishaw and G. M. Mace (2000). Predicting
 460 extinction risk in declining species. *Proc. Roy. Soc. B* **267**, 1947-1952.
 461 Roff, D. (1981). On being the right size. *Am. Nat.* **118**, 405-422.
 462 Salguero-Gómez, R., O. R. Jones, E. Jongejans, S. P. Blomberg, D. J. Hodgson, C.
 463 Mbeau-Ache, P. A. Zuidema, H. De Kroon and Y. M. Buckley (2016). Fast–
 464 slow continuum and reproductive strategies structure plant life-history
 465 variation worldwide. *Proc. Nat. Acad. Sci.* **113**, 230-235.
 466 Smith, M., H. Caswell and P. Mettler-Cherry (2005). Stochastic flood and
 467 precipitation regimes and the population dynamics of a threatened floodplain
 468 plant. *Ecol. Appl.* **15**, 1036-1052.
 469 Stearns, S. C. (1983). The influence of size and phylogeny on patterns of covariation
 470 among life-history traits in the mammals. *Oikos* **41**, 173-187.
 471 Stearns, S. C. (1998). The evolution of life histories, Oxford university press.
 472 Stott, I., S. Townley and D. J. Hodgson (2011). A framework for studying transient
 473 dynamics of population projection matrix models. *Ecol. Letts.* **14**, 959-970.

474 Tuljapurkar, S. (1990). Delayed reproduction and fitness in variable environments.
475 *Proc. Nat. Acad. Sci.* 87, 1139-1143.

476 Tuljapurkar, S. (2013). *Population dynamics in variable environments*, Springer
477 Science & Business Media.

478 White, J. W., C. Barceló, A. Hastings and L. W. Botsford (2022). Pulse disturbances
479 in age-structured populations, Life history predicts initial impact and recovery
480 time. *J. Anim. Ecol.* 91, 2370-2383.

481 Wilbur, H. M. and V. H. Rudolf (2006). Life-history evolution in uncertain
482 environments, bet hedging in time. *Am. Nat.* 168, 398-411.

483 Wright, J., G. H. Bolstad, Y. G. Araya-Ajoy and N. J. Dingemanse (2019). Life-history
484 evolution under fluctuating density-dependent selection and the adaptive
485 alignment of pace-of-life syndromes. *Biol. Rev.* 94, 230-247.

486 Young, W. E. and R. H. Trent (1969). Geometric mean approximations of individual
487 security and portfolio performance. *J. Finance Quant. Anal.* 4, 179-199.

488

489

490

491

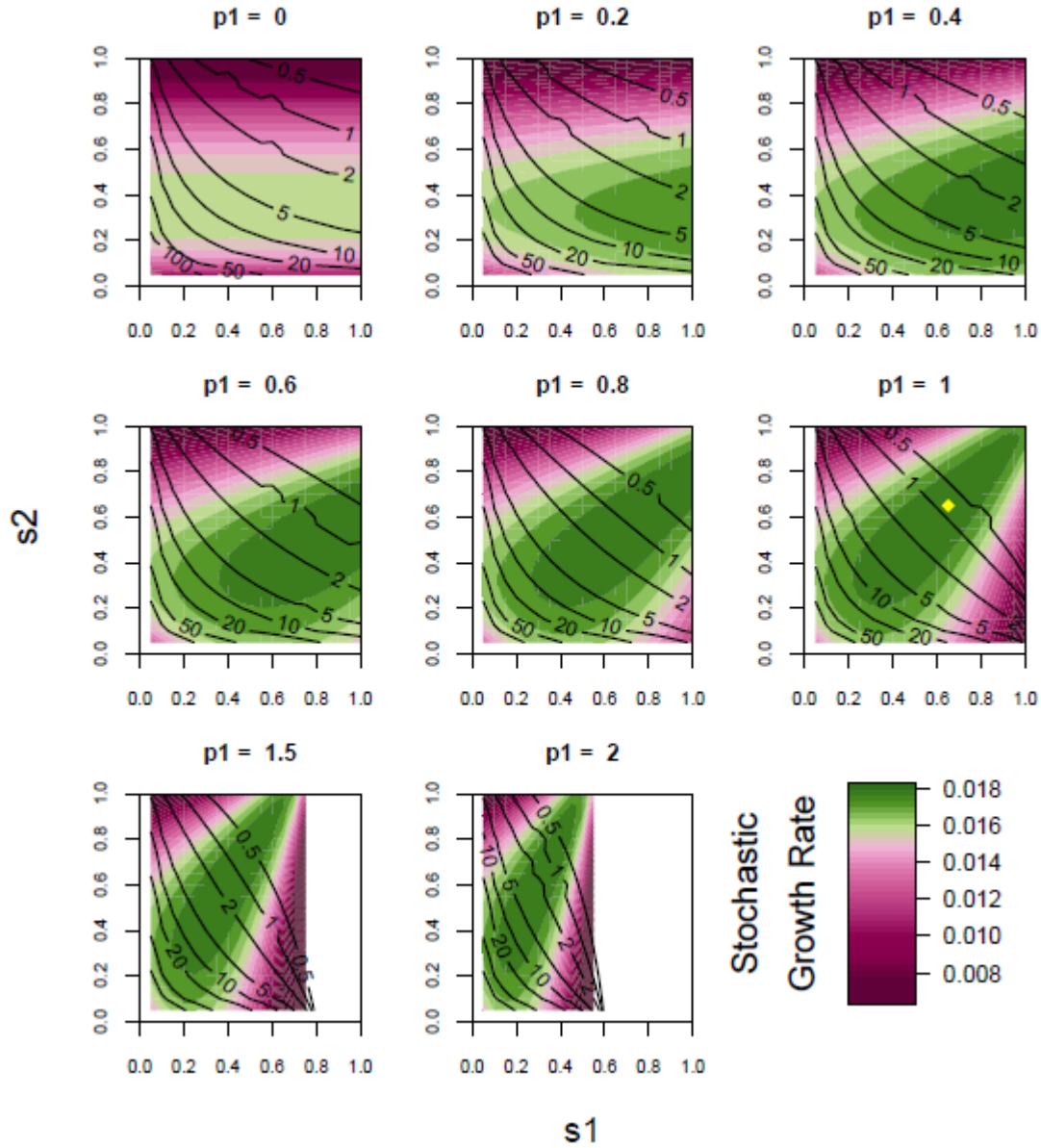


Figure 1: Heatmaps showing the stochastic growth rates (\hat{r}_s) for combinations of adult (s_2) and juvenile (s_1) survival, with contours describing adult productivity (p_2) and panels for different values of juvenile productivity (p_1). All populations disturbed by stage-specific, Uniform-distributed, proportional culls with per-timestep probability $f = 0.2$. The yellow diamond symbol represents the maximum parameter combination over all plots. The areas of block white represent the parameter combinations that are not biologically feasible ($s_1 p_1 > 1.2$).

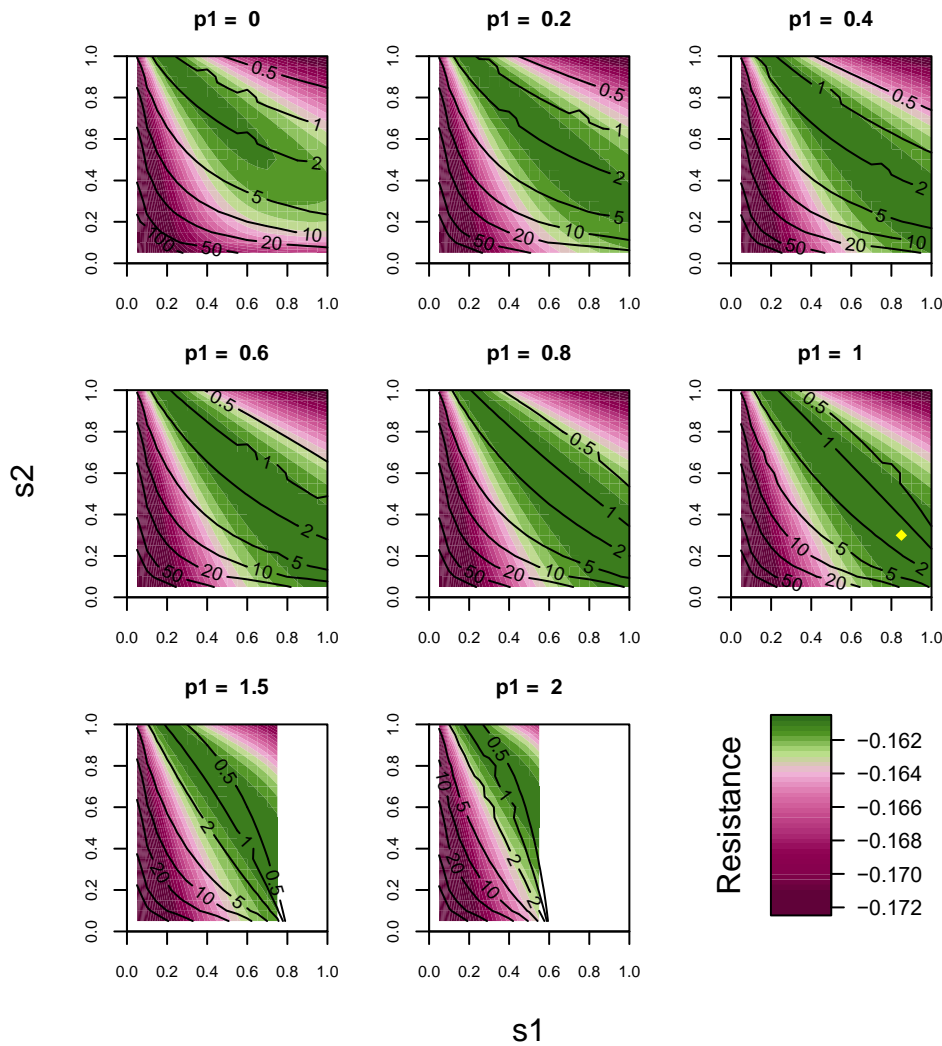


Figure 2: Heatmaps showing demographic resistance, measured as the mean of the log of the ratio of disturbed to undisturbed population size per timestep, for combinations of adult (s_2) and juvenile (s_1) survival, with contours describing adult productivity (p_2) and panels for different values of juvenile productivity (p_1). All populations disturbed by stage-specific, Uniform-distributed, proportional culls with per-timestep probability $f = 0.2$. The yellow diamond symbol represents the maximum parameter combination over all plots.

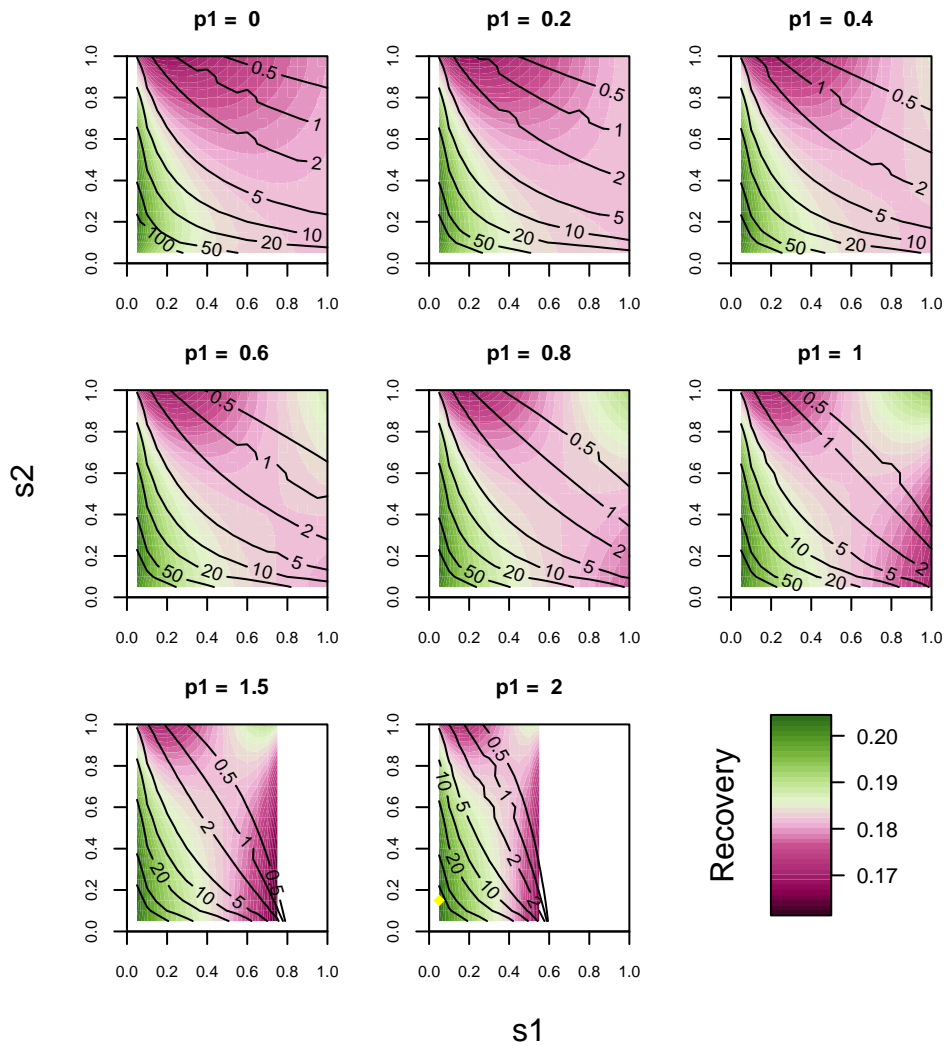


Figure 3: Heatmaps showing demographic recovery, measured as the mean of the log of the ratio of projected to disturbed population size per timestep, for combinations of adult (s_2) and juvenile (s_1) survival, with contours describing adult productivity (p_2) and panels for different values of juvenile productivity. All populations disturbed by stage-specific, Uniform-distributed, proportional culls with per-timestep probability $f = 0.2$. The yellow diamond symbol represents the maximum parameter combination over all plots.

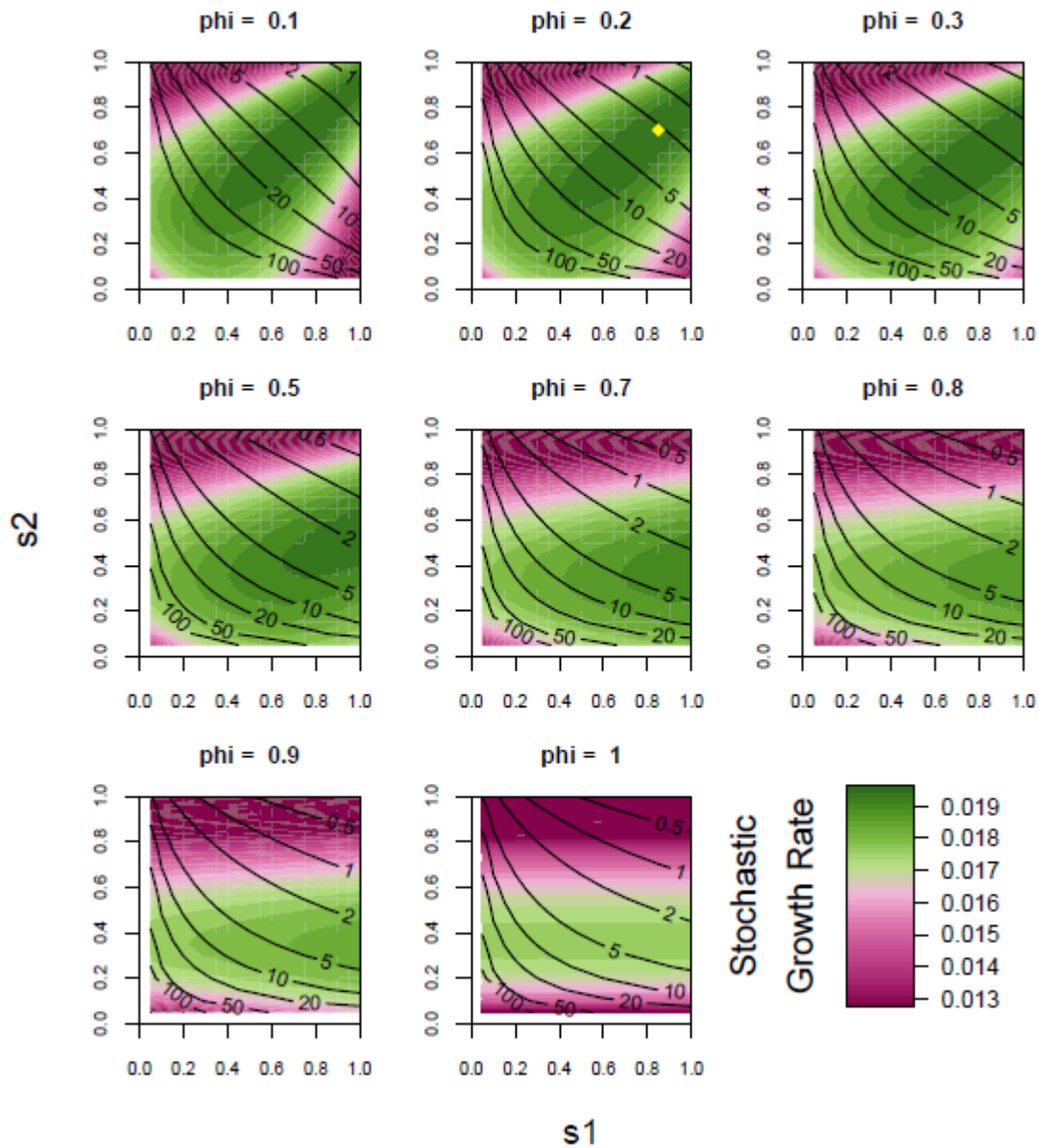


Figure 4: Heatmaps showing the stochastic growth rates (\hat{r}_s) for combinations of adult (s_2) and juvenile (s_1) survival, with contours describing adult productivity (p_2) and panels for different values of maturation rate (ϕ). All populations disturbed by stage-specific, Uniform-distributed, proportional culls with per-timestep probability $f = 0.2$. The yellow diamond symbol represents the maximum parameter combination over all plots.

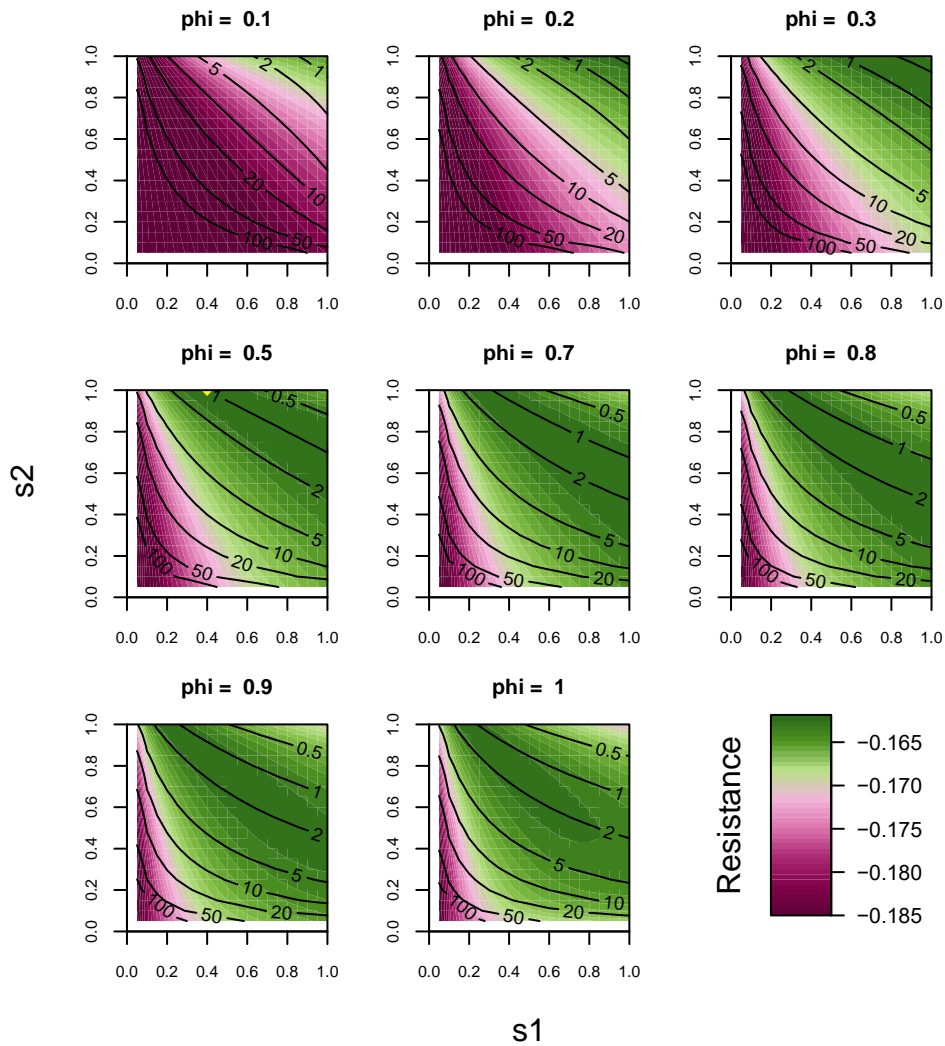


Figure 5: Heatmaps showing demographic resistance, measured as the mean of the log of the ratio of disturbed to undisturbed population size per timestep, for combinations of adult (s_2) and juvenile (s_1) survival, with contours describing adult productivity (p_2) and panels for different values of maturation rate (ϕ). All populations disturbed by stage-specific, Uniform-distributed, proportional culls with per-timestep probability $f = 0.2$. The yellow diamond symbol represents the maximum parameter combination over all plots.

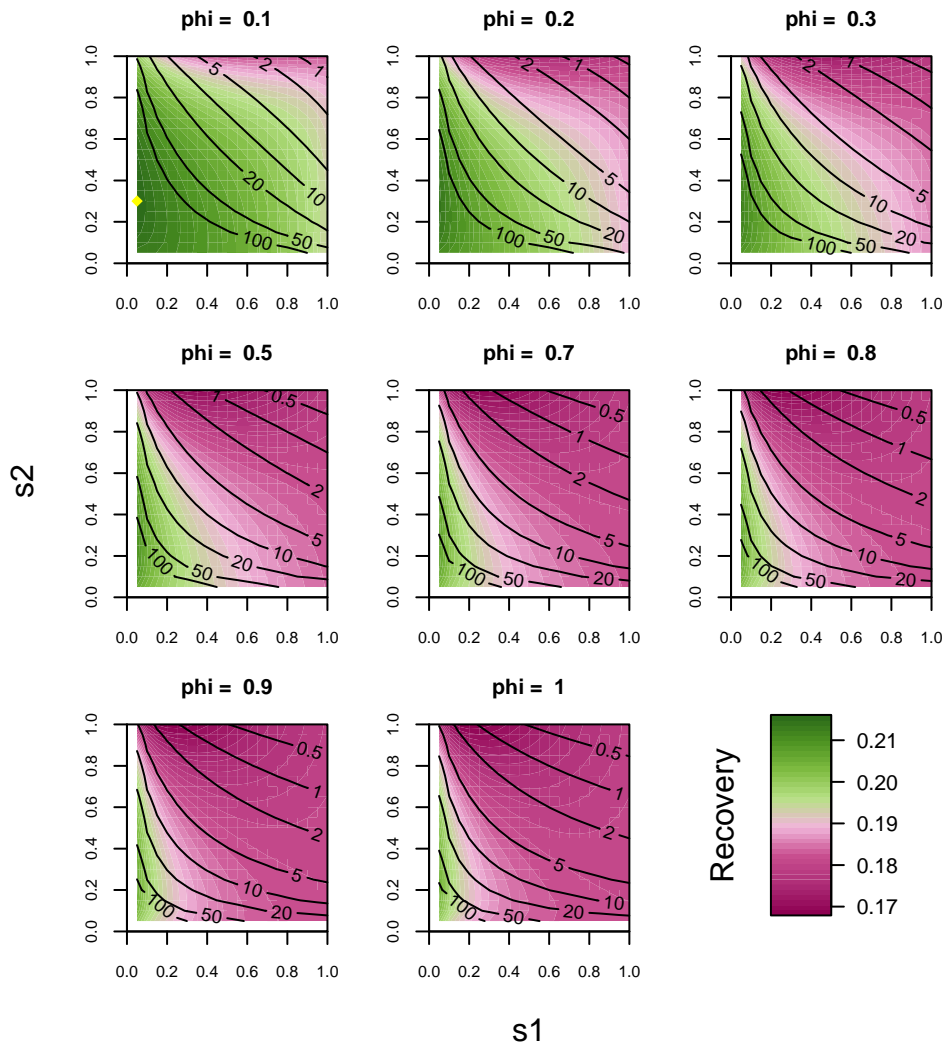


Figure 6: Heatmaps showing demographic recovery, measured as the mean of the log of the ratio of projected to disturbed population size per timestep, for combinations of adult (s_2) and juvenile (s_1) survival, with contours describing adult productivity (p_2) and panels for different values of maturation rate (ϕ). All populations disturbed by stage-specific, Uniform-distributed, proportional culls with per-timestep probability $f = 0.2$. The yellow diamond symbol represents the maximum parameter combination over all plots.

Appendix 1: Why do structured life histories vary in *resistance* to stochastic disturbances?

We have modelled stochastic disturbances as the culling of a Uniform-distributed proportion of members of each age/stage class. The population-level impact of disturbance is therefore the sum across all age/stage-classes following their respective culls. This is the sum of two independent samples from Uniform distributions with bounds defined by 0 below and the abundance of each stage, above.

If we set $n = x_1 + x_2 = 1$ (i.e. working with relative abundance of each age/stage-class), call the stochastic culls U_1 and U_2 , and their combined impact $Z = U_1 + U_2$, we find the pdf of Z is

$$f(z) = \begin{cases} \frac{z}{x_1(1-x_1)}, & \text{for } 0 < z < x_1 \\ \frac{1}{(1-x_1)}, & \text{for } x_1 < z < (1-x_1) \\ \frac{1}{(1-x_1)} + \frac{1}{x_1} - \frac{z}{x_1(1-x_1)}, & \text{for } (1-x_1) < z < 1 \end{cases} \quad [\text{Equation A1.1}]$$

The expected resistance is

$$E(U_1 + U_2) = E(Z) = 0.5 \quad [\text{Equation A1.2}]$$

And its variance is

$$\text{Var}(Z) = \frac{1}{12} - \frac{x_1}{6} + \frac{x_1^2}{6} \quad [\text{Equation A1.3}]$$

Since the expected value of resistance to the combined cull is constant but its variance is quadratic-up in x_1 , the geometric process of multiple culls favours life

histories with even relative abundance of each age/stage (Figure A1). Life histories with stage structures dominated by one stage class, or the other, will be less resistant to stochastic disturbance. This is because the geometric mean gets smaller with constant arithmetic mean and increasing arithmetic variance (Young and Trent 1969, Gillespie 1977). Unbalanced stage structures are typical of the asymmetric projection matrices that describe life histories, hence variation among life histories, in resistance to stochastic disturbances, is not surprising.

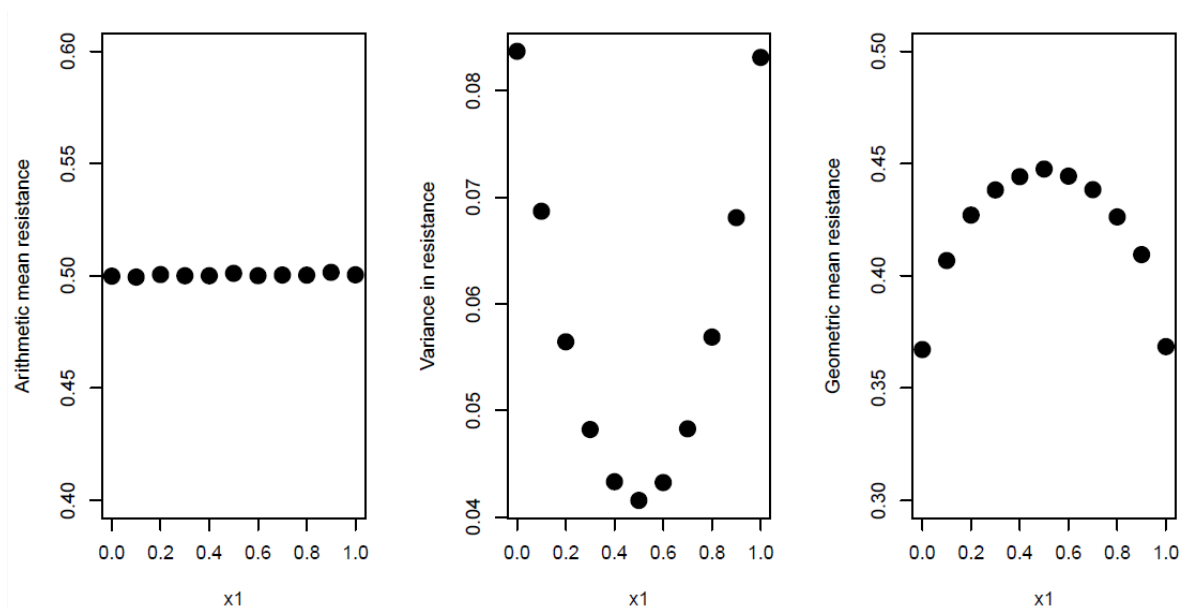


Figure A1: Mean and variance in resistance of 2-stage life histories that vary in the relative abundance (x_1) of the first lifestage. Resistance defined as the instantaneous impact on population abundance caused by Uniform-distributed culling of each lifestage. Means and variances calculated from 100K simulated disturbances. Arithmetic mean resistance is constant, but variance is quadratic in x_1 , and geometric mean (measuring the product of repeated disturbances) peaks at $x_1=0.5$, i.e. is maximised for life histories with even stable stage structure.

Appendix 2: Why do structured life histories vary in *recovery* from stochastic disturbances?

When demographic disturbance pushes age/stage structure away from the stable structure, transient dynamics are invoked while the age/structure settles back to stability through time (Stott, Townley and Hodgson 2011). The only stage structure that grows according to the stable rate of increase is the stable structure. All other stage structures attenuate (have growth rate less than the dominant eigenvalue) or amplify (growth rate greater than the dominant eigenvalue) (Figure A2). In the first timestep following disturbance, if \mathbf{A} is the population projection matrix then abundance will be the 1-norm (sum) of the disturbed stage structure projected through \mathbf{A} :

$$N_{t+1} = \|\mathbf{A}\mathbf{x}_t\|_1 \quad [\text{Equation A2.1}]$$

And the first-timestep rate of recovery, as a multiplier on the stable rate of increase, also known as *reactivity*, is

$$reactivity = \frac{\|\mathbf{A}\mathbf{x}_t\|_1 / \|\mathbf{x}_t\|_1}{\lambda_1(\mathbf{A})} \quad [\text{Equation A2.2}]$$

Recovery will be fastest for life histories constituted by stage classes that are particularly highly productive and/or survive well. These are unlikely to resemble the life histories that are most resistant to disturbance by virtue of having evenly distributed stage structures.

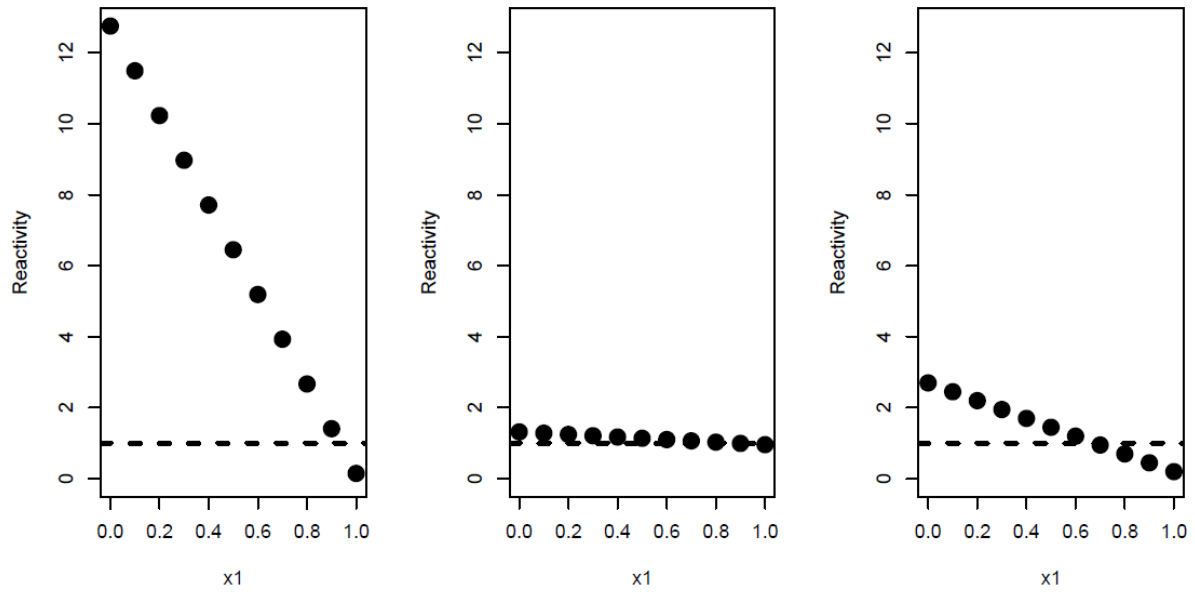


Figure A2: First-timestep recovery from stochastic disturbance for stage structures starting with relative abundance of lifestage 1 (x_1) ranging between 0 and 1, when projected through (a) a fast life history with $\mathbf{A} = \begin{bmatrix} 0.25 & 12.65 \\ 0.1 & 0.1 \end{bmatrix}$; (b) a slow life history with $\mathbf{A} = \begin{bmatrix} 0.16 & 0.52 \\ 0.8 & 0.8 \end{bmatrix}$; (c) a mixed-pace life history with $\mathbf{A} = \begin{bmatrix} 0 & 1.8 \\ 0.2 & 0.9 \end{bmatrix}$. All three life histories have dominant eigenvalue = 1.2, but very different patterns of recovery from demographic disturbance.

Overall we expect a negative association between resistance and recovery, but the relative strength of these two components of resilience will depend on the structure, amplitude and frequency of the disturbance regime, and on the life history described by the projection matrix \mathbf{A} .

610 **Modelling random disturbances in the projection matrix A**

611 Our main description, of findings from demographic disturbance simulations, applied
612 disturbances to population state vectors, allowing us to unpack the relative
613 contributions of demographic resistance and demographic recovery to the resulting
614 stochastic population growth rate or fitness. The usual approach, in stage-structured
615 demographic modelling, is to introduce stochasticity into the demographic system
616 model, in other words into the vital rates that form the population projection matrix.

617 According to equations 5 and 7, the outcome of modelling disturbances as culls of
618 the population state vector, versus modelling them as variation in the vital rates in
619 the population projection matrix, should be identical. Here we present the analogous
620 code and figures that display stochastic population growth rates (AKA fitness) of
621 simple life histories exposed to random disturbances of their vital rates, using Model
622 1: Stage-structured Reproduction. The patterns and measurements in the figures are
623 identical (give or take small noise coming from the simulated disturbance regimes) to
624 Figure 1 in the main manuscript.

625 Hence the findings are indeed equivalent to those shown in the main manuscript.
626 But, by disturbing vital rates instead of culling the population state, we are unable to
627 unpack the relative contributions of demographic resistance and demographic
628 recovery, without recourse to the same algebra used in our culling analysis.

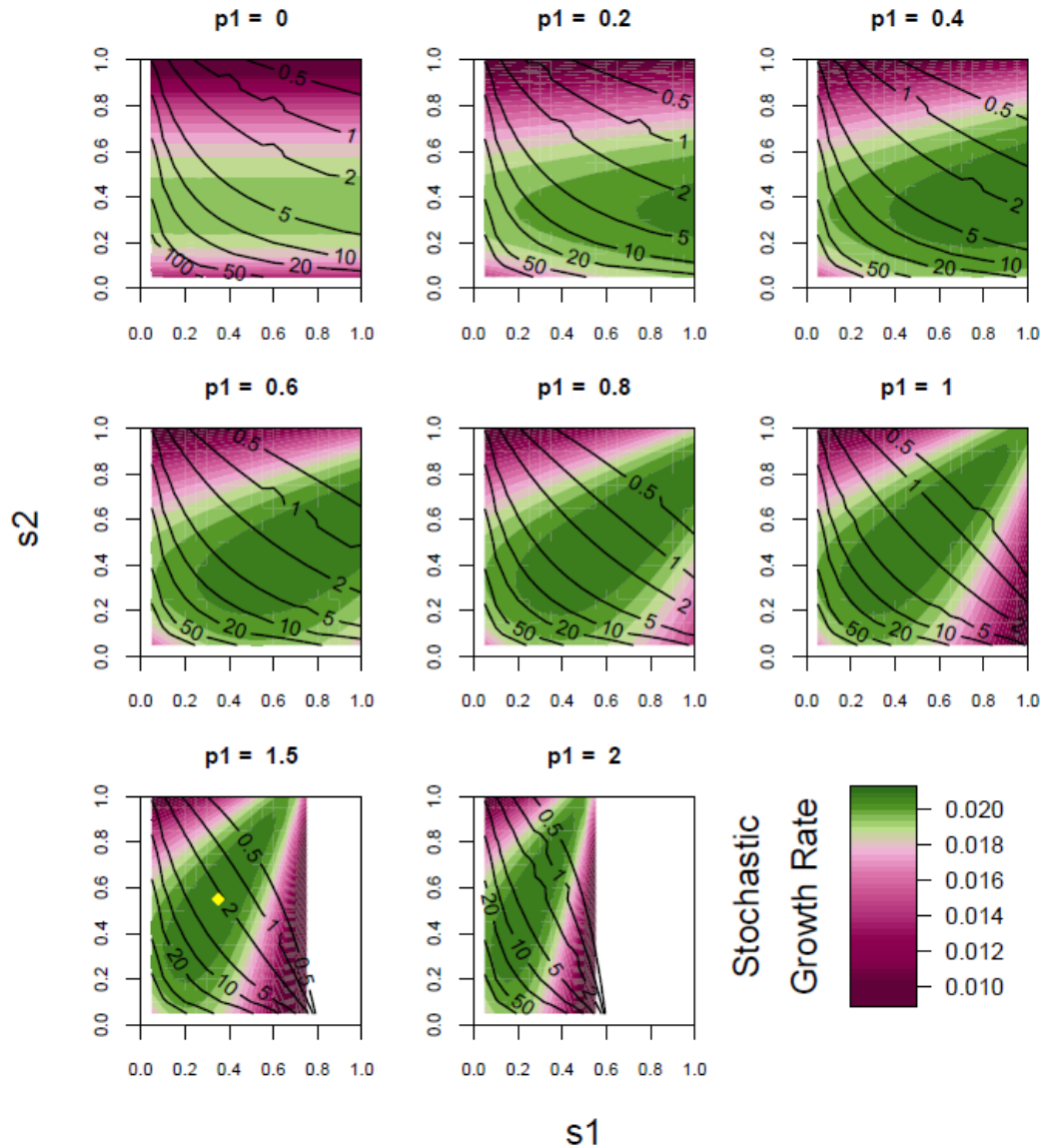


Figure S1: Heatmaps showing the stochastic growth rates (\hat{r}_s) for combinations of adult (s_2) and juvenile (s_1) survival, with contours describing adult productivity (p_2) and panels for different values of juvenile productivity (p_1), when random disturbances are modelled to affect vital rates in the projection matrix **A**. All survival rates disturbed by stage-specific, Uniform-distributed, proportional culls with per-timestep probability $f = 0.2$. The yellow diamond symbol represents the maximum parameter combination over all plots. The areas of block white represent the parameter combinations that are not biologically feasible ($s_1 p_1 > 1.2$).